Temporal evolution of plastic additive contents over the last decades in two major European rivers (Rhone and Rhine) from sediment cores analyses

Alice Vidal, Laure Papillon, Gabrielle Seignemartin, Amandine Morereau, Cassandra Euzen, Christian Grenz, Yoann Copard, Frédérique Eyrolle, Richard Sempéré

Environmental Pollution 348 (2024) 123655

Contents lists available at ScienceDirect

Environmental Pollution

journal homepage: www.elsevier.com/locate/envpol

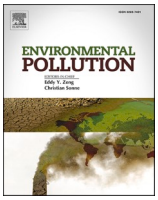

Temporal evolution of plastic additive contents over the last decades in two major European rivers (Rhone and Rhine) from sediment cores analyses☆

Alice Vidal [a,*], Laure Papillon [a], Gabrielle Seignemartin [b], Amandine Morereau [c,d], Cassandra Euzen [e], Christian Grenz [a], Yoann Copard [f], Frédérique Eyrolle [c], Richard Sempéré [a]

[a] Aix Marseille Univ., University of Toulon, CNRS, IRD, MIO UM 110, Marseille, France
[b] Univ. Lyon, Université Claude Bernard Lyon 1, CNRS, ENTPE, UMR5023 LEHNA, F-69518, Vaulx-en-Velin, France
[c] Institut de Radioprotection et de Sureté Nucléaire (IRSN), PSE-ENV, STAAR/LRTA, BP 3, 13115, Saint-Paul-lez-Durance, France
[d] Sorbonne-Université, UMR CNRS, 7619 METIS, 75252, Paris, France
[e] Univ, Strasbourg, CNRS, ENGEES, UMR7362 LIVE, Strasbourg, France
[f] Univ. Rouen Normandie, Université Caen Normandie, CNRS, Normandie Univ, M2C UMR 6143, F-76000, Rouen, France

ARTICLE INFO

Keywords:
Organic plastic additives
Phthalates
Organophosphate esters
River sedimentary archives
Contamination trajectories
Historical pollution

ABSTRACT

Although global plastic distribution is at the heart of 21st century environmental concerns, little information is available concerning how organic plastic additives contaminate freshwater sediments, which are often subject to strong anthropogenic pressure. Here, sediment core samples were collected in the Rhone and the Rhine watersheds (France), dated using ^{137}Cs and $^{210}Pb_{xs}$ methods and analysed for nine phthalates (PAEs) and seven organophosphate esters (OPEs). The distribution of these organic contaminants was used to establish a chronological archive of plastic additive pollution from 1860 (Rhine) and 1930 (Rhone) until today. Sediment grain size and parameters related to organic matter (OM) were also measured as potential factors that may affect the temporal distribution of OPEs and PAEs in sediments. Our results show that OPE and PAE levels increased continuously in Rhone and Rhine sediments since the first records. In both rivers, ∑PAEs levels (from 9.1 ± 1.7 to 487.3 ± 27.0 ng g^{-1} dry weight (dw) ± standard deviation and from 4.6 ± 1.3 to 65.2 ± 11.2 ng g^{-1} dw, for the Rhine and the Rhone rivers, respectively) were higher than ∑OPEs levels (from 0.1 ± 0.1 to 79.1 ± 13.7 ng g^{-1} dw and from 0.6 ± 0.1 to 17.8 ± 2.3 ng g^{-1} dw, for Rhine and Rhone rivers, respectively). In both rivers, di (2-ethylhexyl) phthalate (DEHP) was the most abundant PAE, followed by diisobutyl phthalate (DiBP), while tris (2-chloroisopropyl) phosphate (TCPP) was the most abundant OPE. No relationship was found between granulometry and additives concentrations, while organic matter helps explain the vertical distribution of PAEs and OPEs in the sediment cores. This study thus establishes a temporal trajectory of PAEs and OPEs contents over the last decades, leading to a better understanding of historical pollution in these two Western European rivers.

1. Introduction

Over the last decades, plastic pollution has become a major environmental concern due to its increasing production which was estimated at 390.7 million metric tons in 2021 (Statista Research Department, 2023). Plastics play an important role in the Anthropocene with many being used only once and immediately discarded, most frequently inappropriately. Some of them reach the terrestrial environment and ultimately end up in aquatic environments. Once they reach the aquatic compartment, plastics will be fragmented into smaller sized particles by photodegradation (UV radiation), weathering and physical abrasion (e.g., wind and wave action), as well as by biotic factors (e.g.,

Abbreviations: (TPP), Tripropyl phosphate; (TiBP), Tri-iso-butyl phosphate; (TnBP), Tributyl-n-phosphate; (TCEP), Tris-(2-chloroethyl) phosphate; (TCPP), Tris(2-chloro-1-methylethyl) phosphate; (TCPP-1), Tris(chloroisopropyl) phosphate; (TCPP-2), Bis(2-chloro-1-methylethyl)(2-chloropropyl) phosphate; (TPhP), Triphenyl phosphate; (EHDPP), 2-ethylhexyl diphenyl phosphate; (TEHP), Tri(2-ethylhexyl) phosphate; (TDCP), Tris (1,3-dichloro-2-propyl) phosphate; (TPrP), (TCrP); Tricresyl phosphate, (TDCPP); Tris (1,3-dichloro-2-propyl) phosphate, (TBEP); Tris (2-butoxyethyl) phosphate, (DEP); Diethyl phthalate, (DEHP); Di(2-ethylhexyl) phthalate, (DnBP); Di-n-butyl phthalate, (DMP); Dimethylphthalate, (DiBP); Diisobutyl phthalate, (BBzP), Benzyle butyle phthalate; (DnOP), Di-n-octyl phthalate.

☆ This paper has been recommended for acceptance by Eddy Y. Zeng.

* Corresponding author.
E-mail address: alicevidal@orange.fr (A. Vidal).

https://doi.org/10.1016/j.envpol.2024.123655
Received 24 November 2023; Received in revised form 22 February 2024; Accepted 23 February 2024
Available online 9 March 2024

microorganisms action). Since the beginning of plastic production, a panel of additives have been added to polymers by manufacturers so as to confer particular properties to plastic polymers. Among the organic additives, phthalates (PAEs) and organophosphate esters (OPEs) are the most abundant (Yang et al., 2019). For example, PAEs are used as plasticizers to facilitate processing and to increase the flexibility and the toughness of manufactured plastic products, while OPEs serve as flame retardants and plasticizers (Wang et al., 2020). These chemicals are also added to paints, adhesives, cosmetics and personal care products (Guo and Kannan, 2012), and are subsequently released into the surrounding environment as the products age (Paluselli et al., 2018; Fauvelle et al., 2021). In recent years, studies have highlighted the ecotoxicological concerns of these chemicals for living aquatic organisms (Net et al., 2015; Wei et al., 2015). During riverine transport of organic matter including both natural and anthropogenic compounds, the physico-chemical properties of a myriad of hydrophobic compounds leads them to bind with carbon-rich suspended particulate matter (van der Veen and de Boer, 2012; Net et al., 2015), which then accumulate in the sediment throughout watersheds and in coastal areas (Schmidt et al., 2018; Paluselli et al., 2018). Sedimentary archives from large rivers have been widely explored in recent years (Foucher et al., 2021), and are expected to trace the history of the chemicals introduced by the technological and industrial activities which define the 20th century. However, river sediment cores remain poorly studied for plastics and their additives.

In France, the Rhone and the Rhine are two major rivers most impacted by human activities. They have been strongly modified by the construction of dams, by wastewater treatment plant inputs and by hydro-electrical facilities. Both rivers have previously been studied mainly for the most common heavy metals (e.g. zinc, lead, cadmium, copper) and organic pollutants (e.g. perfluoroalkyl substances, polychlorinated biphenyls, polycyclic aromatic hydrocarbons) (Middelkoop, 2000; Heise and Förstner, 2006; Mourier et al., 2014; Munoz et al., 2015; Mourier et al., 2019; Dendievel et al., 2020; Joerss et al., 2020; Schmidt et al., 2020). More recently, studies reported the presence of plastic additives in freshwater ecosystems. In the sediments of the Rhone River, Alkans et al. (2021) averaged OPE and PAE levels, at 24.9 ± 6.0 ng g^{-1} dry weight (dw) and 69.0 ± 17.4 ng g^{-1} dw, respectively. Paluselli et al. (2017) averaged the PAE concentration in the Rhone River surface water at 615.1 ng.L^{-1}. To the best of our knowledge, the occurrence of OPEs remains unmeasured in the Rhine River, and only Nagorka and Koschorreck (2020) have reported data on PAEs in suspended particulate matter from the Rhine River (>2000 ng g^{-1}). Furthermore, knowledge of historical contamination trends of OPEs and PAEs in riverine sediments remains poor, because few studies precisely date the sediment cores which leads to potential biases regarding the period of time associated with measurements. Understanding the historical trajectories of organic plastic additives in sediment cores is of great importance for estimating the inventory of contaminants that can be associated in part to plastic debris items transferred by rivers to oceans, and for evaluating their impacts on the environment over time. In this context, our study aims to establish the temporal trends of the concentrations of common plastic additives including seven PAEs and nine OPEs by examining dated Rhone and Rhine sediment cores collected at the outlets of watersheds since the beginning of the last century. The grain size distribution as well as organic matter parameters were measured to establish relationships between these key factors and the distribution of OPE and PAE concentrations in the sediments over one century. These results contribute to a better understanding of the plastic additive contamination of freshwater streams, and provide data to implement public policies for environmental risk management.

2. Materials and methods

2.1. Study sites

Sediment core samples were selected in the downstream section of the Rhone and the Rhine rivers in France (Fig. 1) using historical maps, aerial photographs, and both bibliographic and field investigations. Documentary supports allowed to determine as far as was possible, those areas where sedimentary deposition has occurred continuously over the past decades.

The Rhone River stretches for 812 km, originating at the Furka Glacier (2340 m asl) in the Swiss Alps and spanning a 98,500 km^2 watershed with a complex hydrological regime (Olivier et al., 2009). The river flows into the Mediterranean Sea, with an average annual discharge of 1700 m^3 s^{-1} (Olivier et al., 2022) and is the main provider of terrestrial inorganic and organic carbon to the Mediterranean (Sempéré et al., 2000). Throughout the latter half of the 20th century, numerous dams were constructed along the river to satisfy the need for hydroelectric power production, thus transforming the river into a single-thread channel (Tena et al., 2020; Riquier, 2015; Bravard, 2010). Originally initiated by the construction of dike fields and later reinforced by the installation of diversion dams, terrestrialization has led to the deposition of fine sediments, to alterations in water levels, and ultimately, to modifications in the hydrological connection at the margins (Seignemartin et al., 2023). These developments provide context to the Rhone core, revealing sediment deposition in the 1960s within a previously aquatic zone (Fig. 1B). The study site is situated just upstream of the delta and the city of Arles, at the south end of the Lower Rhone segment (Fig. 1A). Its associated drainage area covers 98% of the total watershed area (Fig. 1C).

The Rhine River, which extends for 1233 km, originates in the Swiss Alps at Lake Tomasee. Its watershed covers 185,000 km^2 spanning nine European countries and has an average annual discharge of about 2300 m^3 s^{-1} into the North Sea. The hydrological Rhine regime is nival and the mean annual discharge at the Basel gauging station is 1050 m^3 s^{-1}. During the mid-19th century, the upper Rhine underwent human modifications including channelization efforts for flood control, bank delineation, agricultural advancement, and forest expansion, while dams were constructed in the 20th century (Schmitt, 2001; Arnaud et al., 2015). The Rhine River core originates from the artificial island created by the diversion of the Rhinau dam, built in 1963, in a former braiding and anastomose area that became stabilised due to channelization (Fig. 1B). The drained area associated with the core covers about 20% of the total Rhine watershed, encompassing the entirety of its Swiss and French parts (Fig. 1.A and 1.B).

2.2. Sediment sampling and core dating

Cores were sampled on 11/19/2020 and September 03, 2020 on the Rhone River and on the Rhine River, respectively. Rhone and Rhine cores were collected using a percussion driller (Cobra TT, SDEC, France) with transparent PVC tubes (diameter 46 mm or 100 mm). For the Rhone deposit, which is more than 1 m thick, a master core was obtained by twice sampling successive 1-m sediment cores over less than 1 m^2 surface area. The second coring was vertically shifted by 50 cm compared to the first one in order to preserve sediment samplings from interface disruptions. Once in the laboratory, each 1 m core was cut lengthwise, and slices varying from one to several cm were successively sampled from the surface to the depth, depending on stratigraphy. Slices were stored at −25 °C and freeze-dried under dehydrated nitrogen flux to avoid any atmospheric exchange, and were sieved at 2 mm before analyses.

Sedimentary core samples were analysed by gamma spectrometry. Dry samples were conditioned in 17- or 60-mL tightly closed plastic boxes for gamma counting using low-background and high-resolution Germanium Hyper pure detectors at the IRSN/LMRE laboratory in

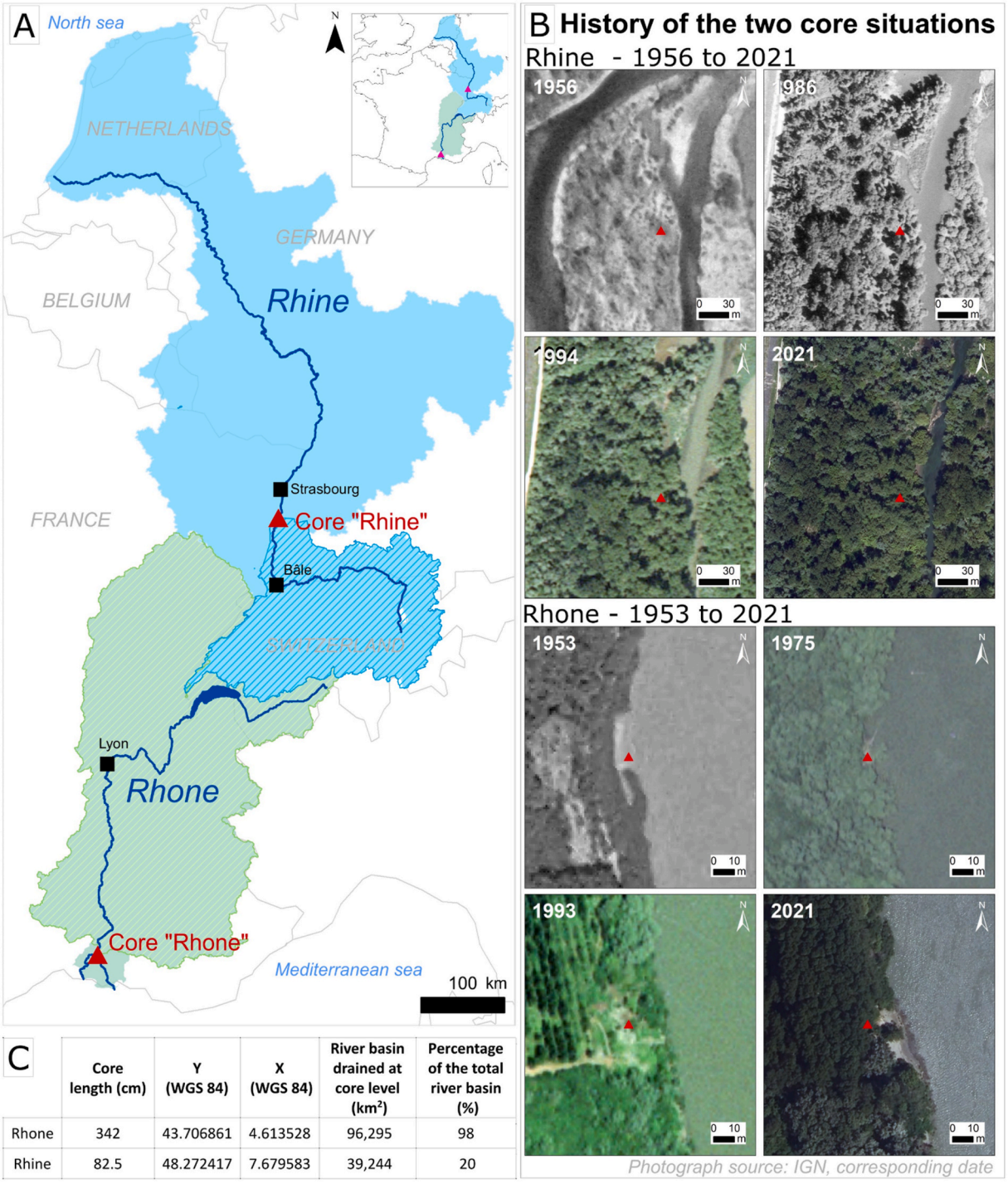

C

	Core length (cm)	Y (WGS 84)	X (WGS 84)	River basin drained at core level (km²)	Percentage of the total river basin (%)
Rhone	342	43.706861	4.613528	96,295	98
Rhine	82.5	48.272417	7.679583	39,244	20

Fig. 1. A. Location of Rhine and Rhone cores with associated drained watersheds (shaded); **B.** Historical evolution of coring sites from aerial photographic archives (photograph source: IGN); **C.** Characteristics of the cores.

Orsay (Bouisset and Calmet, 1997). The boxes were placed in vacuum sealed packages and stored for at least one month before measurement to ensure the secular equilibrium of the ^{210}Pb necessary to determine the concentration of $^{210}Pb_{xs}$ (^{210}Pb in excess). Efficiency calibrations were constructed using gamma-ray sources in a 1.15 g/cm^3 density solid resin–water equivalent matrix. Activity results were corrected for true coincidence summing and self-absorption effects (Lefèvre et al., 2003). Measured activities, expressed in Bq.kg^{-1} dry weight, were decay-corrected to the date of sampling. Activity uncertainty was estimated as the combination of calibration uncertainties, counting statistics, and summing and self-absorption correction uncertainties. A wide range of gamma emissions were detected with a germanium detector including ^{137}Cs, ^{210}Pb and ^{214}Bi used to determine $^{210}Pb_{xs}$. These latter are widely used to date recent sediment deposits (last 100 years) because their half-life allows to cover several decades: 30.08 years for ^{137}Cs and 22.20 years for ^{210}Pb (Goldberg, 1963). Around 30% of sedimentary core samples were additionally analysed by alpha spectrometry after radiochemistry steps to quantify plutonium isotopes (^{238}Pu, ^{239,240}Pu), ^{241}Am and ^{244}Cm. ^{137}Cs and other chronological tracers dating method (method A) and $^{210}Pb_{xs}$ dating method (method B) were detailed in Section S1 (supplementary data), (Eyrolle et al., submitted).

2.3. Sediment grain size distribution

Particle size analyses were carried out on fresh sediment samples using a Beckman Coulter LS 13320 laser micro-particle size analyser (measurement interval between 0.04 and 1813 μm). Each measurement was carried out 3 times (triplicate samples) to reduce heterogeneity uncertainties within the samples, while the d50 and d90 were calculated for each sediment sample and the particle classes were determined according to the classification of Blott and Pye (2001) and processed using Gradistat (Blott, 2000): clay ($x < 2$ μm), silt (2 μm $< x < 63$ μm) and sand ($x > 63$ μm).

2.4. Organic matter parameters

Sedimentary Organic Matter (OM) was characterised using classical bulk organic Rock-Eval 6 pyrolysis (Copard et al., 2006; Baudin et al., 2015), providing total organic carbon (TOC) content and other OM indicators. Such analyses reveal (i) the amount of hydrogenous compounds contained in OM, (ii) the OI (oxygen index, in mg O2.g^{-1} TOC) corresponding to the amount of oxygenated compound contained in OM, (iii) the total organic carbon (TOC, in wt. %) corresponding to the sum of the carbon calculated from pyrolysis and oxidation (RC) steps, (iv) the RC/TOC ratio showing the refractory character of OM and (v) the HI/OI ratio derived from the pyrolysis signals (S2, S3, S3CO) which reveals the global origin and the degradation states of OM (Carrie et al., 2012). S2 (mg of hydrocarbon/g of sample), S3 (mg of CO_2/g of sample) and S3CO (mg of CO/g of sample) are time-integrated signals from pyrolysis step. S2 is referred to the release of hydrocarbon compounds during all the temperature programming. S3 and S3CO are respectively the release of CO_2 and CO from the decomposition of sedimentary OM before 400 °C.

2.5. Extraction and analysis of OPEs and PAEs

All information on chemical and reagent suppliers is detailed in Table S1. Sediment samples were sieved through a pre-cleaned stainless-steel sieve (500 μm diameter) before extraction. All sediment samples were treated with the procedure described by Alkan et al. (2021). Briefly, the sediments samples (3.00 ± 0.05 g dry weight (dw)) were mixed with active copper (1 g) and labelled surrogate standards (10 μL of TBP-d27, TCPP-d18, TDCP-d15, DnBP-d4 at 10 ng mL^{-1}) to monitor the overall extraction efficiency of the target compounds. Cartridges (conditioned with acetone, EtOAc and DCM) containing 250 ± 2.5 mg of Oasis MAX (Waters) sandwiched between two PTFE frits were mounted in a 12-port SPE vacuum Manifold (Supelco, Sigma-Aldrich) for the extraction, three of which corresponded to blanks for each extraction. Two extractions were undertaken: the first with DCM and the second with DCM/EtOAc (70/30). The combined extracts were evaporated to 1 mL under gentle flow using a 12-port Visidry Drying Attachment (Supelco, Sigma-Aldrich). An additional clean-up step was performed by passing the extracts through 3% deactivated alumina (1.5 g) packed in a pre-cleaned Pasteur pipette topped with 0.5 g of sodium sulphate. Finally, the new extract was evaporated (50 μL) into a GC vial. 100 ng of labelled OPE and PAE was added to each sample for the quantification of target compounds, and the extracts were stored at −20 °C until Gas Chromatography – tandem Mass Spectrometry (Triple Quadrupole) (GC-MS/MS (QQQ)) analysis (Agilent 8890 Series GC coupled with an Agilent 7000D TQ), operating in multiple reaction monitoring (MRM) and electron impact (EI, 70 eV) modes. The separation was achieved in a 30 m × 0.25 mm i.d. x 0.25 μm HP-5MS capillary column (Agilent J&W). All target contaminants were quantified according to the internal standard procedure. The injection volume was 2 μL and the helium carrier gas flow was 1 mL min^{-1}. The temperatures of the Mass Selective Detector transfer line and the ion source and quadrupole were set at 150 °C. The following conditions were applied: injector temperature, 270 °C (splitless) and the oven was programmed from 90 °C to 166 °C at 4 °C.min^{-1}, to 175 at 3 °C.min^{-1} (holding time 2 min), to 232 °C at 4 °C.min^{-1}, to 290 °C at 10 °C.min^{-1} and then to 310 °C at 10 °C.min^{-1} (holding time 7.4 min). The total duration of one sample analysis was thus 53.45 min.

2.6. Cross-contamination from the coring

Additional analyses were performed to quantify the levels of OPEs and PAEs introduced by the PVC made-corer itself, despite the permanent and rigorous aspiration during the coring stage and the precautions taken during each of the treatment steps. An experimental blank sediment sample was therefore baked at 450 °C for 6h to eliminate any potential trace of additives and was rewet with ultra-pure water. Blank sediment was introduced into the PVC-made corer and the same treatment was applied as for the experimental samples. Three replicates of blank sediment were collected at the end of the whole procedure. All replicates were then treated to extract the additives (OPEs and PAEs) and were analysed following the same methodology as for the experimental sediment samples. The cross-contamination was quantified for each PAE and each OPE (Table S2). Finally, to homogenize the results and allow a comparison between the two rivers, the given concentrations were first corrected by the recoveries, then blank concentrations and concentrations from cross-contamination were subtracted.

2.7. Quality assurance/quality control

Strict measures were taken to prevent potential cross contamination during OPE and PAE analysis. First, the use of plastic material was avoided at all times and all glassware was cleaned overnight with detergent, rinsed with tap water + MQ water and then baked at 450 °C for 6 h before use. Alumina and sodium sulphate were also baked overnight at 450 °C before use. Sample treatment and extraction/clean-up steps were performed entirely in an International Standards Organization (ISO) 6 cleanroom (22 °C, SAS + 15 Pa cleanroom pressure, 50 vol.h^{-1} brewing rate) (Paluselli et al., 2018). The retention time and the response factors of GC-MS/MS (QQQ) were evaluated for each analytical sequence by regularly injecting different calibration levels. One hexane injection was performed every 3 samples to check and monitor potential cross contamination along the sequence. In addition, all samples analysed were spiked with labelled surrogates. The average recoveries and the mean blank values are presented in Table S3. All concentrations of PAE and OPE (ng.g^{-1}) presented in this study have been corrected by subtracting the corresponding mean blank value and the concentration introduced by the coring.

2.8. Statistical analysis

Pearson correlations were performed using data related to organic matter (TOC, RC/TOC, S2, S3, S3CO3 and HI/OI), granulometry (d10, d50 and d90), and PAE and OPE concentrations for Rhone and Rhine sediment samples in order to evaluate the relationships between the sediment grain size, OM, and plastic additive concentrations over time. Pearson correlation coefficients were performed with the Rstudio application associated with R software (version 4.3.1).

3. Results

3.1. Age/depth models based on ^{137}Cs and alpha emitters chronological tracers, and $^{210}Pb_{xs}$ profiles

Our results show that along the Rhine sedimentary core, ^{137}Cs mainly peaks at 21 cm depth (91.1 Bq.kg^{-1}) while all alpha emitters (^{238}Pu, ^{239,240}Pu, ^{241}Am, ^{244}Cm) peak at around 27 cm (Fig. S1). These maximums can be attributed to the years 1986 (Chernobyl accident) and 1963 (Atmospheric global fallout for nuclear tests), respectively, whereas the drastic ^{137}Cs activity decrease towards detection limits below 41 cm indicates that the pre-bomb test period was reached in

1955. The sandy strata at 75–80 cm depth corresponds probably to extreme flood events after the beginning of the correction works (Euzen et al., submitted). Additionally, Euzen et al. (submitted) reported an additional chronological benchmark at 80 cm depth attributed to the year 1882. The use of all these chronological tracers gives calculated apparent sedimentation rates (ASR) of 0.5, 1.8, 0.3 and 0.6 cm.y^{-1} for the 1882–1955, 1955–1963, 1963–1986 and 1986–2021 periods, respectively, which is in line with estimations obtained using the $^{210}Pb_{xs}$ approach (Table S4, Figs. S1 and S2).

The Rhone core results show increasing ^{137}Cs activities starting from 250.5 cm depth, which can be attributed to the 1955 nuclear events (Fig. S1). Activities of ^{137}Cs and artificial alpha emitters vary towards maximum values of between 139 and 233 cm, highlighting the releases from the spent fuel reprocessing plant. Those releases were the most important over the 1963–1990 period and partially mask the Chernobyl accident contribution (Eyrolle et al., 2008; Provansal et al., 2010). By using these chronological benchmarks, mean ASR are 3.8, 3.5 and 4.5 cm.y^{-1} for the periods 1955–1963, 1963–1990 and 1990–2020, respectively. These values are very close to those calculated over the 1930–2020 period using the $^{210}Pb_{xs}$ method, i.e. 3.8 cm.y^{-1} (Fig. S1). A mean apparent sedimentation rate of 3.8 cm.y^{-1} can therefore be extrapolated here for the pre-1955 period.

3.2. Grain-size sediment distribution

Our results show that silts make up most of the sedimentary particles in both rivers, with an exception at around 260 cm depth in the Rhone core where sands are seen to dominate (Fig. 2). These sedimentary layers, corresponding to the 1950s in the Rhone core, probably highlight one or several major flood events (flow rates in the range of 7760–9180 m^3 s^{-1}). Interestingly, the small but significant increase of amounts of sand around 15, 60 and 150 cm depth may indicate traces of the great floods of 1993/94, 11/26/2002 and March 12, 2003, and of 11/23/2016, respectively. These sedimentary layers can be dated to these periods by our model, reinforcing the age/depth model acquired for the Rhone core.

Amounts of sands are in general significantly higher in the Rhone core when compared to the Rhine, most probably due to (i) the specific hydro-sedimentary characteristics of the rivers, (ii) deposition environments and conditions, and (iii) the vicinity of the Rhone coring point to the water flow of the river (<5 m) when compared to the Rhine system (>50 m). Finally, the d90 versus d50 diagram (Fig. S3) indicates sedimentary deposits mainly constituted after settling of uniform suspension, which most generally characterises the dominance of clay and silts in riverine sediments. These results underline that the two sediment cores studied are rather similar regarding the grain size of sedimentary deposits, and that particles deposited are generally rather similar over time.

3.3. Organic matter parameters

For both sediment cores, our results showed that TOC content ranged from 0.33% to 4.63% for the Rhine River and from 0.64% to 2.63% for the Rhone River (Table 1). TOC remained relatively constant with depth for the Rhone River but decreased for the Rhine River. The RC/TOC ratio ranged from 0.65 to 0.76 for the Rhine River and from 0.74 to 0.91 for the Rhone River. Other parameters (S2, S3, S3CO and HI/OI) were higher for the Rhine River than for the Rhone River (Table 1).

3.4. Environmental levels of PAEs and OPEs in Rhone and Rhine sediments

Levels of PAEs and OPEs were both higher in Rhine sediment cores (Fig. 3A and C) than in Rhone cores (Fig. 3B and D), at *ca.* ten times higher for PAEs and four times higher for OPEs. Clearly, PAEs and OPEs concentrations increased over time from the first records to the most recent dates, with higher levels of PAEs (Fig. 3C and D) than OPEs (Fig. 3A and B), in both rivers. For both rivers, the trajectory of the plastic additive contamination is more obvious and linear for OPEs than for PAEs. Indeed, the concentrations of some PAEs can be seen to peak at times, then to decrease before rising again. However, for both categories of plastic additives, the first noticeable contamination appears in sediment dated around 1963, followed by a significant increase reported post-2000 (Fig. 3).

3.5. Relative abundances of PAEs and OPEs in sediments of the Rhone and Rhine rivers

Interestingly, TPP was never detected in Rhone and Rhine sediment cores, and TiBP, TnBP, TDCP (OPEs) and DEP (PAE) were not detected in Rhone sediments (Fig. 3E, F and 3G, Tables S5, S6, S7 and S8). By contrast, several additives were quantified in all layers of sediment cores: these include DiBP, DnBP, BBzP and DnOP in both rivers, DEHP, DEP, DMP (PAEs, Fig. 3G and H), TDCP and TEHP (OPEs, Fig. 3E and F) in the Rhine River, and TCPP in the Rhone River. In Rhone samples, EHDPP and DMP were quantified only in one or two middle layers, and TPhP only in upper layers. TPhP was also detected only in upper layers of Rhine sediments, with TnBP. Finally, some additives were measured in upper and middle layers: TiBP, TCEP, TCPP and EHDPP for the Rhine, and TCEP, TEHP and DEHP for the Rhone.

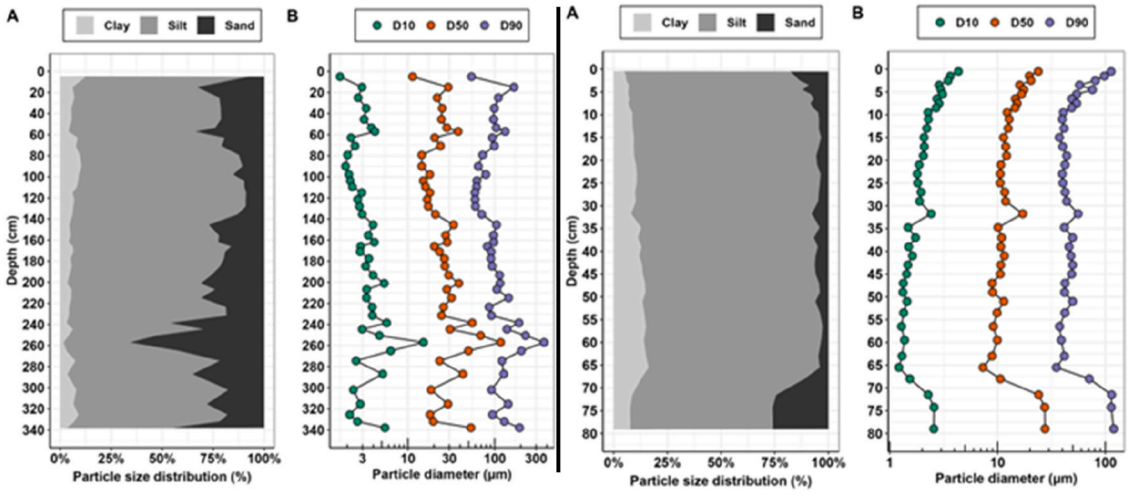

Fig. 2. Particle size distribution (A) and diameter (B) of the sediment core samples of the Rhone River (left) and Rhine River (right).

Table 1
Proportion of total organic carbon in studied sediment core samples (TOC%), ratio of residual carbon to total organic carbon (RC/TOC), hydrocarbons (S2, S3, S3CO) and the ratio of the index of hydrogens to the index of oxygens (HI/OI) for the Rhone and the Rhine sediment core samples.

Rhone							Rhine						
Sample	TOC(%)	RC/TOC	S2	S3CO	S3	HI/OI	Sample	TOC(%)	RC/TOC	S2	S3CO	S3	HI/OI
2020	1.01	0.79	1.62	0.34	1.79	1.08	**2020.4**	4.63	0.65	15.06	2.52	8.6	1.95
2017	2.63	0.74	5.86	1.06	4.62	1.48	**2017.1**	4.3	0.68	12.09	1.87	7.98	1.75
2013.9	1.29	0.79	2.06	0.53	2.15	1.1	**2013.7**	3.25	0.7	8.22	1.57	6.63	1.44
2011.2	1.47	0.8	2.25	0.57	2.35	1.1	**2010.3**	3.07	0.7	7.64	1.46	6.35	1.4
2006.5	0.94	0.83	1.06	0.29	1.64	0.78	**2007**	3.22	0.71	7.58	1.54	7.27	1.23
2002.4	0.64	0.82	0.76	0.21	1.29	0.71	**2002.3**	3.14	0.71	7.26	1.54	6.79	1.25
1995.6	0.99	0.82	1.17	0.32	1.9	0.75	**1996.1**	2.74	0.71	6.47	1.39	5.81	1.29
1989.1	1.45	0.83	1.79	0.45	2.36	0.9	**1989.4**	2.44	0.72	5.46	1.15	5.26	1.22
1979.2	0.89	0.83	0.98	0.26	1.64	0.73	**1978.3**	1.91	0.72	4.34	0.93	4.44	1.15
1962.6	1.29	0.91	0.84	0.21	1.36	0.76	**1963**	1.63	0.72	3.61	0.8	3.65	1.16
1959.5	0.8	0.88	0.62	0.15	1.09	0.71	**1960.3**	1.41	0.74	2.83	0.76	3.31	1
1957.8	0.59	0.85	0.52	0.15	1.02	0.63	**1957.3**	1.03	0.74	2	0.46	2.42	0.99
1956.2	0.7	0.89	0.47	0.11	0.99	0.6	**1947.5**	0.62	0.71	1.37	0.28	1.4	1.16
1946	0.76	0.86	0.73	0.18	1.16	0.77	**1940**	0.53	0.75	0.95	0.25	1.28	0.88
1938.1	1.18	0.9	0.87	0.18	1.15	0.93	**1909.1**	0.74	0.76	1.34	0.35	1.73	0.92
1931.8	0.75	0.83	0.87	0.21	1.17	0.9	**1897.9**	0.33	0.73	0.72	0.15	0.59	1.4
							1860	0.45	0.76	0.77	0.25	0.91	0.96

In Rhine sediment samples, TCPP and TEHP appeared to be the most abundant OPEs whereas DEHP followed by DiNP were the predominant PAEs. In the Rhone samples, TCPP and DEHP were also the most abundant OPE and PAE, respectively. Prior to 1963, only one OPE (TCPP) was detected in Rhone sediments, yet it was quantified only after 1963 in the Rhine, which presented TEHP, TDCP and TiBP in sediments before that date. For PAEs, DEHP appeared from 1909 in the Rhine, but was quantified only much later (1979) in the Rhone. Before these dates, DiBP, DnBP, BBzP and DNoP were reported in sediments of both rivers, and DMP and DEP additionally in the Rhine.

3.6. Relationship between plastic additive levels, organic matter and granulometry

Correlations between levels of each PAE, each OPE, total OPEs (ΣOPEs), total PAEs (ΣPAEs), with data related to OM (TOC, HI/OI, S2, S3 and S3CO) and granulometry (d10, d50 and d90) for the Rhine are quite similar to those for the Rhone (Fig. 4 and S4). Data related to granulometry was not correlated with plastic additive levels. However, for both rivers, parameters related to OM were correlated with levels of OPEs and PAEs, while RC/TOC ratio was anti-correlated with those concentrations. Furthermore, concentrations of individual OPE and total OPEs presented stronger correlations with OM than did concentrations of individual PAE or total PAEs. Correlations between variables were stronger for the Rhine than for the Rhone. For the Rhine, TCPP, TDCP, EHDPP, TEHP and ΣOPEs, and DMP, BBzP, DEHP, DnOP and ΣPAEs all showed strong positive correlations with all OM parameters (>0.6) except with RC/TOC. For the Rhone, only TCPP, ΣOPEs, DEHP and ΣPAEs presented quite strong positive correlations with all OM parameters (>0.5) except with RC/TOC.

4. Discussion

Historically, Western European River contamination trends of OPEs and PAEs has been poorly documented, with most of the existing studies omitting to date the sediment cores (Paluselli et al., 2018; Schmidt et al., 2020; Alkan et al., 2021; Nagorka and Koschorreck, 2020). Yet establishing the trajectories of plastic additives in sediment archives is of great importance for the reconstruction of environmental and human exposures to these contaminants over the last decades. Such approaches applied to plastics additives are scarer and mechanisms involved in their sequestration are poorly documented. Plastic additives are hydrophobic substances that undoubtedly react with solid particles since they are largely encountered in the riverine, coastal and marine sedimentary compartments. In this study, the detection of OPEs and PAEs in sediment cores sampled in the Rhine and the Rhone rivers is reported since the earliest dates recorded (1860 and 1931, respectively). In these old years, OPEs and PAEs were probably not used as additives for plastics but in other applications. Also, a contamination in this study cannot be excluded. Apart from the temporal trends observed and discussed hereafter, relatively high levels during some short periods of time suggest periodic and localised historical pollution events. Data on additive production volume during the earlier years is not available at the scale of the studied watersheds, but van der Veen and de Boer (2012) demonstrated that OPEs have been employed worldwide for up to 150 years and that PAEs have been used since the beginning of the 20th century. Today, they are in the class of synthetic chemicals with high production volumes and toxicological properties (Schecter et al., 2013).

Temporal trends of OPE levels. The contamination profiles of OPEs are similar for both rivers, with low concentrations before 1960, then increasing to finally reach the highest concentrations in the 2000s. These results are consistent with the history of OPEs, which were first introduced in the early 1900s with a rapid increase after the 1940s (USEPA, 1986). After early 21st century, the use of OPEs expanded significantly worldwide following the ban on polybrominated diphenyl ethers (Stapleton et al., 2012). As an example, in 2018, 1.05 million tons of OPEs were used globally (Z.C. Group, 2018). Cao et al. (2017) investigated the contamination of OPEs in dated sediment cores from Lake Michigan (USA) and reported concentrations of alkyl- (sum of TMP, TEP, TPrP, TiBP, TnBP, TBEP, and TEHP) and chlorinated (sum of TCEP, TCPP, and TDCP) OPEs from 1860 until the 2000s. However, existing studies reporting vertical distribution and historical contamination trends of OPEs in sediments have received little attention (Luo et al., 2023). Some studies reviewed by Wang et al. (2020) showed concentrations of OPEs in surface sediments sampled in Europe which are similar to those reported in this study. Indeed, mean levels of ΣOPEs in several European rivers were measured at dozens to hundreds of $ng.g^{-1}$, including rivers in Spain (Cristale et al., 2013), Austria (Martínez-Carballo et al., 2007), Germany (Stachel et al., 2005) and three European river basins (Adige, Evrotas and Sava) (Giulivo et al., 2017). In the coastal NW Mediterranean Sea, Alkan et al. (2021) reported $\sum_9$OPE concentrations from surface sediments sampled in 2018 in the Rhone River (Gulf of Lion) that ranged from 4 to 227 ng g^{-1} dw (mean: 54 ng g^{-1} dw).

In our study, TCPP was the dominant OPE in both rivers. A similar trend has been observed in other studies: Zhang et al. (2018) found that TCPP was one of the dominant OPEs in the microplastics collected from coastal beaches in China, accounting for 35.1%, and Ma et al. (2022)

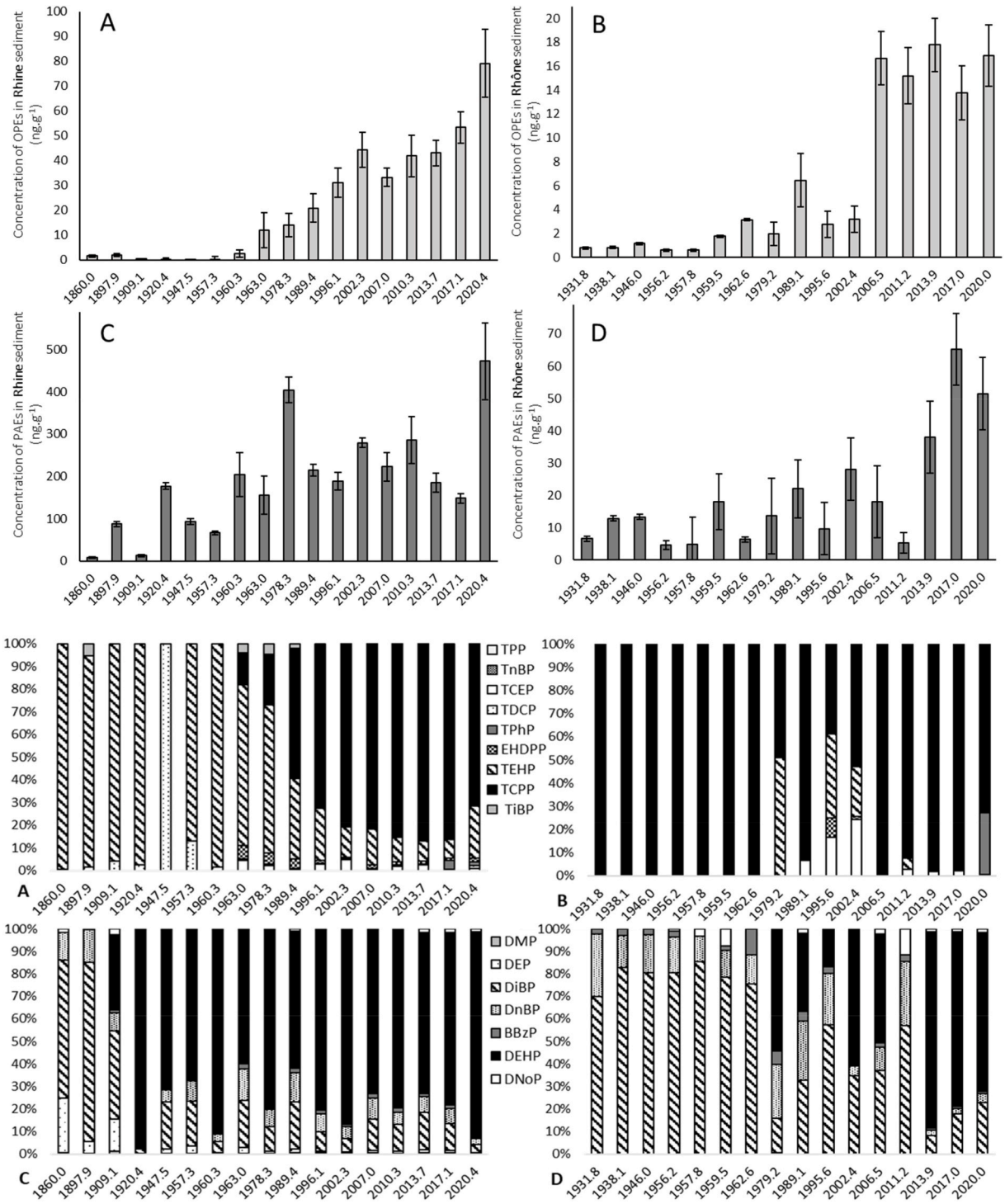

Fig. 3. Concentrations (ng.g^{-1} dw) of OPEs (A and B) and PAEs (C and D), and relative abundances of individual OPE (E and F) and PAE (G and H) measured in sediment core samples of the Rhine River (A and C) and the Rhone River (B and D).

also found TCPP as the dominant OPE in sediments of the Dong Nai River (Vietnam), with an average contribution of 81%. Temporal trends observed by Cao et al. (2017) demonstrated that the recent increase in depositional flux to sediment is dominated by chlorinated OPEs, especially TCPP. TCPP levels reported in our study also suggest historical contamination, since the chemical was detected from 1931 in the Rhone River and from slightly later in the Rhine River, in 1963. This can be explained by the high production volume of TCPP and its common uses as a flame retardant to comply with flammability standards for rigid and spray polyurethane foam (building insulation), and for flexible polyurethane foam (furniture and automotive seating) (Babrauskas et al., 2012; van der Veen and de Boer, 2012). Due to the fact that TCPP is added but not chemically bonded to polymers, it can be released into the environment through volatilization, abrasion, and dissolution in addition to through direct contact with dust and surfaces (Rauert et al., 2014). Moreover, the concentrations of TEHP were dominant in the Rhine River compared to other OPEs and have continued to increase since the first record in 1860. TEHP, an alkyl-OPE, is usually added to paints, coatings and textiles (Chen and Ma, 2021; van der Veen and de Boer, 2012) but is not generally the most abundant OPE in

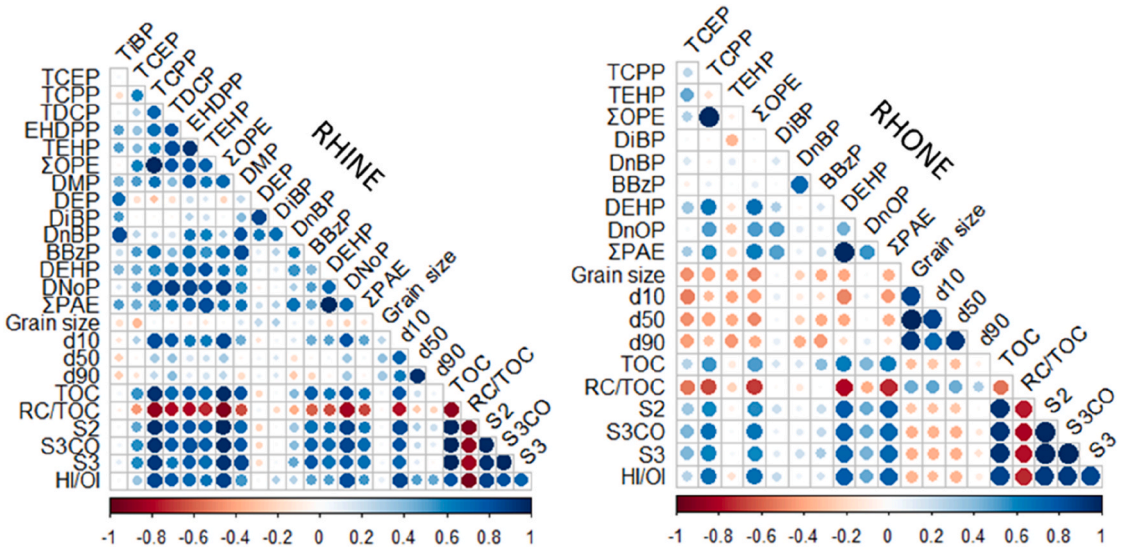

Fig. 4. Pearson correlations of the levels of each PAE, each OPE, grain size, d10, d50, d90 and all organic matter factors (TOC, RC/TOC, S2, S3, S3CO and HI/OI ratio) of sediment core samples of Rhine and Rhone rivers. The red circles correspond to anti-correlations while the blue ones correspond to correlations. The larger the diameter of the circles, the stronger the correlations. (For interpretation of the references to colour in this figure legend, the reader is referred to the Web version of this article.)

environmental samples. However, some studies have also measured high TEHP concentrations compared to other OPEs. For example, Sutton et al. (2019) reported higher TEHP concentrations in sediments of San Francisco Bay (median concentrations of 8.2 ng g^{-1} dw) than other analysed phosphate flame retardants (TCrP, TPhP, TDCPP and TBEP). In the surface sediment samples of the Scheldt Estuary (Holland), TEHP ranged from 0.4 to 3.3 ng g^{-1} dw (Brandsma et al., 2015). TEHP was found to range from 0.620 ng g^{-1} dw to 7.90 ng g^{-1} dw in the Dong Nai River System (Vietnam) (Ma et al., 2022), revealing levels that are comparable to the measurements reported in this paper. TEHP is hydrophobic with high logKow and may be strongly adsorbed by the sediments with high TOC content (Van der Veen and De Boer, 2012; Ma et al., 2022), which corroborates results from the Rhine River.

Finally, the pattern of OPEs was more diverse in Rhine sediments than in those of the Rhone. Despite the same order of magnitude of the concentrations of ∑OPEs compared to our study, Cao et al. (2017) found a more diverse profile of OPEs, with TCPP, TiBP, TnBP measured in sediments of their three studied lakes before the 1900s. Ma et al. (2022) demonstrated that human activities had a clear impact on the patterns and spatial distribution of OPEs in sediments. The nature of industrial activities that developed at the scale of the catchment upstream of the sampling points may thus explain the differences in diversity of OPEs between the Rhine and Rhone rivers.

Temporal trends of PAE levels. In 2009, worldwide PAE production stood at 6.2 million tons (He et al., 2019), of which a large amount is likely to be found in aquatic ecosystems. As is the case for OPEs, historical contamination of PAEs in sediments is still poorly documented. In this study, some PAEs from the first record (1860 and 1931, respectively) were measured at non-negligible concentrations in the Rhine and Rhone rivers, suggesting long-term contamination. Kang et al. (2016) showed historical contamination of some PAEs, dating DiBP and DnBP detected in Lake Chaohu sediments (China) to 1849. In addition to the historical contamination shown in our study, the unpredictable profile of ∑PAE levels in sediments over time with peaked concentrations at some dates, suggests localised and intermittent pollution of both rivers. What is more, the levels of PAEs remains higher than OPEs in both the Rhine and the Rhone. This is consistent with Alkan et al. (2021), who reported a maximum concentration of ∑PAEs at 766 ng g^{-1} dw in surface sediments of the Rhone River (Gulf of Lion), while that of ∑OPEs reached 227 ng g^{-1} dw. Schmidt et al. (2021) also highlighted that PAEs (12–610 ng g^{-1} dw) concentrations were generally higher than OPEs (13–49 ng g^{-1} dw) in sediments collected from three different sampling stations in Marseille Bay (France).

Among all PAEs, DEHP is always present in the environment and has been dominant for decades in sediment samples in most cases (Bergé et al., 2013). Chen et al. (2018) detected DEHP in all sediment samples of the Love River (China), with concentrations between 4.2 and 66.7 ng g^{-1} dw, indicating that it is a common pollutant in the river's environment. Their results are close to those found for the Rhone River in this study, although they are about ten times higher in the Rhine River. Alkan et al. (2021) also found that DEHP was the most abundant PAE, representing an average of 67% of the ∑PAEs. This occurrence is explained by the widespread applications of DEHP and by the fact that DEHP weakly binds with plastics. As a result, large amounts of DEHP may be being released into the environment directly from plastic materials and products (Chen et al., 2018). Despite existing alternatives to DEHP, such as diisononyl phthalate (DiNP) or diisodecyl phthalate (DiDP) (not studied in this work), this chemical remains present in various environmental matrices (Net et al., 2015). Considering that DEHP is highly sensitive to contamination during sampling, transport and analysis, it cannot be ruled out that our samples may be slightly contaminated, despite the precautions taken at all steps of the study and the estimated blank consideration. High DiBP and DnBP concentrations were also found in the Rhone and the Rhine rivers, which is in agreement with what has already been reported from the bottom to the surface in Lake Chaohu (China) core sediments (Kang et al., 2016). This is probably due to its high production and use around the world (Kang et al., 2016). Indeed, DnBP was primarily used in agricultural plastic film until being banned in 2000, while DiBP is still widely used as a plasticizer and softener in the plastics industry. Due to this, DiBP constitutes one of the most common organic contaminants detected worldwide (Kang et al., 2016). Despite European regulations implemented since 2000 which ban products containing certain phthalates such as DEHP or DnBP, concentrations of PAEs found in aquatic environments remain alarming.

Influence of sediment grain size and organic matter parameters on PAEs and OPEs levels. The influence of sediment grain size and organic matter on the levels of plastic additives also remains poorly documented. However, it is expected that high specific surface area of grain sediment, most generally enriched in OM, induces higher adsorption of

hydrophobic organic pollutants (Jaffé, 1991). Given that OM tends to adsorb on fine grains, a higher content of pollutants is commonly observed in this case (Chen et al., 2018; Ma et al., 2022). In addition to the different histories of urbanisation of the two rivers, the higher plastic additive concentrations found in the Rhine River may be explained by the river's higher proportion of fine sediments (Fig. 2). However, in this study, no correlation between sediment grain size and plastic additive levels was highlighted by the Pearson correlations, excluding this last hypothesis and suggesting that the temporal distribution of OPEs and PAEs is not disrupted by the grain size. The grain size of archived particles is over all very similar and reflect close hydrodynamic conditions during the sedimentary particle settling. This suggests that the deposition of microplastic particles, if directly involved in plastics additive contents, was also driven from comparable processes and do not interfere on the temporal trends of plastic additives.

OM parameters were found in some cases to play an important role in the behaviour and the fate of plastic additives in the environment, even though the few existing reports in the literature put forward some controversial conclusions for both PAEs and OPEs. In the present study, the strong correlations observed in some cases between OPEs, PAEs contents and OM indicators suggest that OM and additives content sources are associated at certain periods, likely in relation with terrestrial runoff. This can be most convincingly hypothesized in the case of the Rhine core, where OPE and PAE contents generally decreased with depth similarly to TOC contents. Nevertheless, such similar trends with depth between OPEs, PAEs and OM were not observed for the Rhone cores, where TOC contents are rather constant with depth unlike OPEs and PAEs, excluding the first hypothesis.

For PAEs, Xiang et al. (2019) concluded that the sorption of dibutyl phthalate (DBP) was inversely associated with soil particle sizes, and Xu and Li (2008) concluded that OM in sediments is essential to explain the DBP adsorption capacity. The correlation analysis performed by Chen et al. (2018) showed that grain size and OM may play a key role in DEHP distribution in the sediments during the dry season, whereas DEHP concentrations in the wet season may be principally affected by other environmental and hydrological conditions (transport, mixing and sedimentation mechanisms). Finally, Kang et al. (2016) found that the contents of ΣPAEs, as well as of individual PAEs (DMP, DEP, DiBP, DnBP, DEEP, DBEP, and DnOP) in sediment cores, were significantly positively correlated with the percentage of sand particles and, contrariwise, negatively correlated with the percentage of fine particles. They also highlighted the significantly positive relationship between TOC and the contents of ΣPAEs, as well as low-molecular-weight PAEs (DMP, DEP, DIBP, DnBP, DEEP).

Concerning the OPEs, Luo et al. (2020) found not only that the distribution pattern of ΣOPEs in different particle-size fractions is irregular and varies with the land-use types, but also that correlations between total OPEs or individual OPE concentrations versus TOC are weak. However, Ma et al. (2022) showed that the concentrations of TCPP and TEHP exhibit a significant moderate positive correlation with TOC, while TCPP showed no correlation with grain size, and TEHP presented a significant correlation with clay and silt, as well as showing a significant anti-correlation with sand. This corroborates the fact that OPEs with low water solubility such as TEHP, EHDPP and TPhP, TnBP and TiBP preferentially absorbed onto particulate OM (Martínez-Carballo et al., 2007). Compounds with higher logKow or higher logKoc values were more easily adsorbed by sediments, while OPEs with logKoc >5 were almost completely associated with sediment particles (Cao et al., 2017; Ma et al., 2022). Other factors such as physicochemical properties, emission intensity and degradation may play a role in some instances (Ma et al., 2022). Herein, positive and significant correlations between plastic additive levels and OM parameters occur essentially with the pyrolyzed C (S2, S3, S3CO), while the negative correlations occur with the refractory C (RC/TOC). Accordingly, the sorption process appears to concern the labile fraction of sedimentary OM which exhibits chemical functional groups such as CH2, CH3 (e.g methyl) for hydrogen and COH, CO (alcohol, ketone, ester) for oxygen. The additives studied here are potentially degradable in sediment like the rest of the organic compounds, with very probably different kinetics. It is important to note that the presence of contaminants such as OPEs can, in addition, induced a decrease on the diversity of the bacterial community (as number of microbial species) as has been demonstrated for OPEs in the coastal Mediterranean marine sediment (Castro-Jiménez et al., 2022). This modification could very likely influence the degradation kinetics of natural organic matter. While some relationships between plastic additives and organic matter contents were highlighted in our study no information on the link with microplastic contents is currently available neither from our study nor the literature. In this context, the origin of plastics additives in sedimentary archives needs further investigation to be clearly identified, in particular the relations with microplastics contents.

5. Conclusion

Concentrations of ∑9OPEs and ∑7PAEs have increased continuously since temporal records reconstructed from sediment cores began to be kept, i.e. since 1860 for the Rhine River and 1930 for the Rhone River. Referring to the earliest comparative periods, the data acquired herein show elevated concentrations since the 1990s and even higher values since the 2000s. No correlation was seen between sediment grain size and plastic additive levels, while some parameters related to OM, such as TOC, were shown to correlate with OPEs and PAEs contents without disruption of temporal trends. The results of this study highlight the environmental changes that occurred during the last industrial era and reveal how the memory of riverine sediments provides a useful record for reporting environmental impacts related to human activities. This study also suggests that when incorporated into studies involving neural networks, our data may be helpful for establishing relationships between the levels of contamination observed in sedimentary archives and anthropogenic pressures. Finally, our results will contribute towards better protection of aquatic environments and the development of a management strategy concerning plastic additives.

CRediT authorship contribution statement

Alice Vidal: Writing – review & editing, Writing – original draft, Formal analysis, Data curation. **Laure Papillon:** Methodology, Formal analysis, Data curation. **Gabrielle Seignemartin:** Methodology, Data curation. **Amandine Morereau:** Formal analysis, Data curation. **Cassandra Euzen:** Investigation, Formal analysis. **Christian Grenz:** Writing – review & editing. **Yoann Copard:** Writing – review & editing, Methodology, Formal analysis. **Frédérique Eyrolle:** Writing – review & editing, Supervision, Methodology, Funding acquisition. **Richard Sempéré:** Writing – review & editing, Supervision.

Declaration of competing interest

The authors declare that they have no known competing financial interests or personal relationships that could have appeared to influence the work reported in this paper.

Data availability

Data will be made available on request.

Acknowledgements

The authors are grateful to the ANR TRAJECTOIRE project (ANR-19-CE3- 0009, 2020–2024) for financial support and warmly thank Francois Chabaux (Université de Strasbourg, Laboratoire d'HYdrologie et de GEochimie de Strasbourg (LHyGeS), UMR 7517, École et Observatoire des Sciences de la Terre (EOST)), Laurent Schmitt and Dominique

Babariotti (Université de Strasbourg, Laboratoire Image Ville Environnement (LIVE), UMR 7362, Faculté de Géographie et d'Aménagement), Hugo Lepage, Valérie Nicoulaud-Gouin, Franck Giner, David Mourier, Xavier Cagnat and Anne De Vismes (Institut de Radioprotection et de Sureté Nucléaire (IRSN)), François Baudin (ISTeP laboratory, Sorbonne Université for RE6 analyses).

Appendix A. Supplementary data

Supplementary data to this article can be found online at https://doi.org/10.1016/j.envpol.2024.123655.

References

Alkan, N., Alkan, A., Castro-Jiménez, J., Royer, F., Papillon, L., Ourgaud, M., Sempéré, R., 2021. Environmental occurrence of phthalate and organophosphate esters in sediments across the Gulf of Lion (NW Mediterranean Sea). Sci. Total Environ. 760, 143412 https://doi.org/10.1016/j.scitotenv.2020.143412.

Arnaud, F., Piégay, H., Schmitt, L., Rollet, A.J., Ferrier, V., Béal, D., 2015. Historical geomorphic analysis (1932–2011) of a by-passed river reach in process-based restoration perspectives: the old Rhine downstream of the kembs diversion dam (France, Germany). Geomorphology 236, 163–177. https://doi.org/10.1016/j.geomorph.2015.02.009.

Babrauskas, V., Lucas, D., Eisenberg, D., Singla, V., Dedeo, M., Blum, A., 2012. Flame retardants in building insulation: a case for re-evaluating building codes. Build. Res. Inf. 40, 738–755. https://doi.org/10.1080/09613218.2012.744533.

Baudin, F., Disnar, J.-R., Aboussou, A., Savignac, F., 2015. Guidelines for Rock–Eval analysis of recent marine sediments. Org. Geochem. 86, 71–80. https://doi.org/10.1016/j.orggeochem.2015.06.009.

Bergé, A., Cladière, M., Gasperi, J., Coursimault, A., Tassin, B., Moilleron, R., 2013. Meta-analysis of environmental contamination by phthalates. Environ. Sci. Pollut. Res. Int. 20, 8057–8076. https://doi.org/10.1007/s11356-013-1982-5.

Blott, S., 2000. GRADISTAT Version 4.0. Surrey.

Blott, Simon J., Pye, Kenneth, 2001. Gradistat: a grain size distribution and statistics package for the analysis of unconsolidated sediments. Earth Surf. Process. Landforms 26, 1237–1248. https://doi.org/10.1002/esp.261.

Bouisset, P., Calmet, D., 1997. Hyper pure gamma-ray spectrometry applied to low-level environmental sample measurements. In: International Workshop on the Status of Measurement Techniques for the Identification of Nuclear Signatures. Geel, Belgium.

Brandsma, S.H., Leonards, P.E., Leslie, H.A., de Boer, J., 2015. Tracing organophosphorus and brominated flame retardants and plasticizers in an estuarine food web. Sci. Total Environ. 505, 22–31.

Bravard, J.P., 2010. Discontinuities in braided patterns: the River Rhone from Geneva to the Camargue delta before river training. Geomorphology 117, 219–233. https://doi.org/10.1016/j.geomorph.2009.01.020.

Cao, D., Guo, J., Wang, Y., Li, Z., Liang, K., Corcoran, M.B., et al., 2017. Organophosphate esters in sediment of the great lakes. Environ. Sci. Technol. 51 (3), 1441–1449. https://doi.org/10.1021/acs.est.6b05484.

Carrie, J., Sanei, H., Stern, G., 2012. Standardisation of Rock–Eval pyrolysis for the analysis of recent sediments and soils. Org. Geochem. 46, 38–53. https://doi.org/10.1016/j.orggeochem.2012.01.011.

Castro-Jiménez, J., Cuny, P., Militon, C., et al., 2022. Effective degradation of organophosphate ester flame retardants and plasticizers in coastal sediments under high urban pressure. Sci. Rep. 12, 20228 https://doi.org/10.1038/s41598-022-24685-6.

Chen, M., Ma, W., 2021. A review on the occurrence of organophosphate flame retardants in the aquatic environment in China and implications for risk assessment. Sci. Total Environ. 783, 147064 https://doi.org/10.1016/j.scitotenv.2021.147064.

Chen, C.F., Ju, Y.R., Lim, Y.C., Chang, J.H., Chen, C.W., Dong, C.D., 2018. Spatial and temporal distribution of di-(2-ethylhexyl) phthalate in urban river sediments. Int J Environ Res Public Health 15 (10), 2228. https://doi.org/10.3390/ijerph15102228, 11.

Copard, Y., Di-Giovanni, C., Martaud, T., Albéric, P., Olivier, J.E., 2006. Using Rock-Eval 6 pyrolysis for tracking fossil organic carbon in modern environments: implications for the roles of erosion and weathering. Earth Surf. Process. Landforms 31, 135–153. https://doi.org/10.1002/esp.1319.

Cristale, J., Vazquez, A.G., Barata, C., Lacorte, S., 2013. Priority and emerging flame retardants in rivers: occurrence in water and sediment, Daphnia magna toxicity and risk assessment. Environ. Int. 59, 232–243.

Dendievel, A.M., Mourier, B., Dabrin, A., Delile, H., Coynel, A., Gosset, A., Liber, Y., Berger, J.F., Bedell, J.P., 2020. Metal pollution trajectories and mixture risk assessed by combining dated cores and subsurface sediments along a major European river (Rhone River, France). Environ. Int. 144, 106032 https://doi.org/10.1016/j.envint.2020.106032.

Eyrolle, F., Claval, D., Gontier, G., Antonelli, C., 2008. Radioactivity level in major French rivers: summary of monitoring chronicles acquired over the past thirty years and current status. J. Environ. Monit. 10, 800–811.

Euzen, C., Chabaux, F., Rixhon, G., Preusser, F., Eyrolle, F., Badariotti, D., Schmitt, L. Combining Geochronological Methods Improves Accuracy of Young Floodplain Sediment Dating. Submitted.

Fauvelle, V., Garel, M., Tamburini, C., et al., 2021. Organic additive release from plastic to seawater is lower under deep-sea conditions. Nat. Commun. 12, 4426. https://doi.org/10.1038/s41467-021-24738-w.

Foucher, A., Chaboche, P.A., Sabatier, P., Evrard, O., 2021. A worldwide meta-analysis (1977–2020) of sediment core dating using fallout radionuclides including 137Cs and 210Pbxs. Earth Syst. Sci. Data 13, 4951–4966. https://doi.org/10.5194/essd-13-4951-2021,2021.

Giulivo, M., Capri, E., Kalogianni, E., Milacic, R., Majone, B., Ferrari, F., Eljarrat, E., Barceló, D., 2017. Occurrence of halogenated and organophosphate flame retardants in sediment and fish samples from three European river basins. Sci. Total Environ. 586, 782–791. https://doi.org/10.1016/j.scitotenv.2017.02.056.

Goldberg, E.D., 1963. Geochronology with 210-Pb. Radioact. Dating 121–131.

Group, Z.C., 2018. In-depth Investigation and Investment Prospect Analysis Report of China's Flame Retardant Market in 2014–2018. Zhiyan Consulting Group.

Guo, Y., Kannan, K., 2012. Challenges encountered in the analysis of phthalate esters in foodstuffs and other biological matrices. Anal. Bioanal. Chem. 404, 2539–2554. https://doi.org/10.1007/s00216-012-5999-2.

He, Y., Wang, Q., He, W., Xu, F., 2019. The occurrence, composition and partitioning of phthalate esters (PAEs) in the water-suspended particulate matter (SPM) system of Lake. Sci. Total Environ. 661, 285–293. https://doi.org/10.1016/j.scitotenv.2019.01.161.

Heise, S., Förstner, U., 2006. Risks from historical contaminated sediments in the rhine basin. Water Air Soil Pollut. 6, 625–636.

Jaffé, R., 1991. Fate of hydrophobic organic pollutants in the aquatic environment: a review. Environ. Pollut. 69, 237–257. https://doi.org/10.1016/0269-7491(91)90147-O.

Joerss, H., Schramm, T.R., Sun, L., Guo, C., Tang, J., Ebinghaus, R., 2020. Per- and polyfluoroalkyl substances in Chinese and German river water - point source- and country-specific fingerprints including unknown precursors. Environ. Pollut. 267, 115567 https://doi.org/10.1016/j.envpol.2020.115567.

Kang, L., Wang, Q.M., He, Q.S., et al., 2016. Current status and historical variations of phthalate ester (PAE) contamination in the sediments from a large Chinese lake (Lake Chaohu). Environ. Sci. Pollut. Res. 23, 10393–10405. https://doi.org/10.1007/s11356-015-5173-4.

Lefèvre, O., Bouisset, P., Germain, P., Barker, E., Kerlau, G., Cagnat, X., 2003. Self-absorption correction factor applied to 129I measurement by direct gamma–X spectrometry for Fucus serratus samples. Nucl. Instrum. Methods Phys. Res. 506 (1–2), 173–185.

Luo, Q., Wu, Z., Gu, L., 2020. Distribution pattern of organophosphate esters in particle-size fractions of urban topsoils under different land-use types and its relationship to organic carbon content. Arch. Environ. Contam. Toxicol. 79, 208–218. https://doi.org/10.1007/s00244-020-00747-6.

Luo, Q., Wang, C., Gu, L., Wu, Z., Li, Y., 2023. Temporal trends of organophosphate esters in a sediment core from the tidal flat of Liao River estuary, Northeast China. Front. Mar. Sci. 10, 1160371 https://doi.org/10.3389/fmars.2023.1160371.

Ma, Y., Saito, Y., Ta, T.K.O., Li, Y., Yao, Q., Yang, C., Nguyen, V.L., Gugliotta, M., Wang, Z., Chen, L., 2022. Distribution of organophosphate esters influenced by human activities and fluvial-tidal interactions in the Dong Nai River System, Vietnam. Sci. Total Environ. 812, 152649.

Martínez-Carballo, E., Gonzalez-Barreiro, C., Sitka, A., Scharf, S., Gans, O., 2007. Determination of selected organophosphate esters in the aquatic environment of Austria. Sci. Total Environ. 388 (1–3), 290–299.

Middelkoop, H., 2000. Heavy-metal pollution of the river Rhine and Meuse floodplains in The Netherlands. Neth. J. Geosci. 79, 411–427. https://doi.org/10.1007/S0016774600021910.

Mourier, B., Desmet, M., Van Metre, P.C., Mahler, B.J., Perrodin, Y., Roux, G., Bedell, J. P., Lefèvre, I., Babut, M., 2014. Historical records, sources, and spatial trends of PCBs along the Rhone River (France). Sci. Total Environ. 476–477, 568–576. https://doi.org/10.1016/j.scitotenv.2014.01.026.

Mourier, B., Labadie, P., Desmet, M., Grosbois, C., Raux, J., Debret, M., Copard, Y., Pardon, P., Budzinski, H., Babut, M., 2019. Combined spatial and retrospective analysis of fluoroalkyl chemicals in fluvial sediments reveal changes in levels and patterns over the last 40 years. Environ. Pollut. 253, 1117–1125. https://doi.org/10.1016/j.envpol.2019.07.079.

Munoz, G., Giraudel, J.L., Botta, F., Lestremau, F., Dévier, M.H., Budzinski, H., Labadie, P., 2015. Spatial distribution and partitioning behavior of selected poly- and perfluoroalkyl substances in freshwater ecosystems: a French nationwide survey. Sci. Total Environ. 517, 48–56. https://doi.org/10.1016/j.scitotenv.2015.02.043.

Nagorka, R., Koschorreck, J., 2020. Trends for plasticizers in German freshwater environments - evidence for the substitution of DEHP with emerging phthalate and non-phthalate alternatives. Environ. Pollut. 262, 114237 https://doi.org/10.1016/j.envpol.2020.114237.

Net, S., Sempéré, R., Delmont, A., Paluselli, A., Ouddane, B., 2015. Occurrence, fate and behavior and ecotoxicological state of phthalates in different environmental matrices. Environ. Sci. Technol. 49, 4019–4035. https://doi.org/10.1021/es505233b.

Olivier, J.M., Dole-Olivier, M.J., Amoros, C., Carrel, G., Malard, F., Lamouroux, N., Bravard, J.P., 2009. Chapter 7 - the rhône river basin. In: Tockner, K., Uehlinger, U., Robinson, C.T. (Eds.), Rivers of Europe. Academic Press, pp. 247–295. https://doi.org/10.1016/B978-0-12-369449-2.00007-2.

Olivier, J.M., Carrel, G., Lamouroux, N., Dole-Olivier, M.J., Malard, F., Bravard, J.P., Piégay, H., Castella, E., Barthélemy, C., 2022. Chapter 7 - the Rhone River basin. In: Tockner, K., Zarfl, C., Robinson, C.T. (Eds.), Rivers of Europe, second ed. Elsevier, pp. 391–451.

Paluselli, A., Aminot, Y., Galgani, F., Net, S., Sempéré, R., 2017. Occurrence of phthalate acid esters (PAEs) in the northwestern Mediterranean Sea and the Rhone River. Prog. Oceanogr 163, 221–232. https://doi.org/10.1016/j.pocean.2017.06.002.

Paluselli, A., Fauvelle, V., Schmidt, N., Galgani, F., Net, S., Sempéré, R., 2018. Distribution of phthalates in Marseille Bay (NW Mediterranean Sea). Sci. Total Environ. 621, 578–587. https://doi.org/10.1016/j.scitotenv.2017.11.306.

Provansal, M., Villiet, J., Eyrolle, F., Raccasi, G., Gurriaran, R., Antonelli, C., 2010. High-resolution evaluation of recent bank accretion rate of the managed Rhone: a case study by multi-proxy approach. Geomorphology 117, 287–297.

Rauert, C., Lazarov, B., Harrad, S., Covaci, A., Stranger, M., 2014. A review of chamber experiments for determining specific emission rates and investigating migration pathways of flame retardants. Atmos. Environ. 82, 44–55. https://doi.org/10.1016/j.atmosenv.2013.10.003.

Riquier, J., 2015. Réponses hydrosédimentaires de chenaux latéraux restaurés du Rhône français. Université de Lyon, France.

Schecter, A., Lorber, M., Guo, Y., Wu, Q., Yun, H.S., Kannan, K., Hommel, M., Imran, N.S. L., Cheng, D.H., Colacino, J.A., Birnbaum, L.S., 2013. Phthalate concentrations and dietary exposure from food purchased in New York state. Environ. Health Perspect. 121, 473–479.

Schmidt, N., Castro-Jiménez, J., Fauvelle, V., Sempéré, R., 2018. Zooplankton and plastic additives—insights into the chemical pollution of the low-trophic level of the mediterranean marine food web. In: Proceedings of the International Conference on Microplastic Pollution in the Mediterranean Sea. Springer Water. Springer, Cham. https://doi.org/10.1007/978-3-319-71279-6_17.

Schmidt, N., Castro-Jimenez, J., Fauvelle, V., Sempéré, R., 2020. Plastic organic additives in the Rhone River (France) surface waters – a one-year monitoring study. Env. Pol. 257, 113637 https://doi.org/10.1016/j.envpol.2019.113637.

Schmidt, N., Castro-Jimenez, J., Oursel, B., Sempéré, R., 2021. Phthalates and organophosphate esters in surface water, sediments and zooplankton of the NW Mediterranean Sea: exploring links with microplastic abundance and accumulation in the marine food web. Environ. Pollut. 272, 115970 https://doi.org/10.1016/j.envpol.2020.115970.

Schmitt, L., 2001. Typologie hydro-géomorphologique fonctionnelle de cours d'eau : Recherche méthodologique appliquée aux systèmes fluviaux d'Alsace (These de doctorat). Université Louis Pasteur, (Strasbourg), pp. 1971–2008.

Seignemartin, G., Mourier, B., Riquier, J., Winiarski, T., Piégay, H., 2023. Dike fields as drivers and witnesses of twentieth-century hydrosedimentary changes in a highly engineered river (Rhone River, France). Geomorphology 431, 108689. https://doi.org/10.1016/j.geomorph.2023.108689.

Sempéré, R., Charrière, B., van Wambeke, F., Cauwet, G., 2000. Carbon inputs of the rhône river to the Mediterranean Sea: biogeochemical implications. Global Biogeochem. Cycles 14, 669–681. https://doi.org/10.1029/1999GB900069.

Stachel, B., Jantzen, E., Knoth, W., Kruger, F., Lepom, P., Oetken, M., Reincke, H., Sawal, G., Schwartz, R., Uhlig, S., 2005. The Elbe flood in August 2002 - organic contaminants in sediment samples taken after the flood event. J. Environ. Sci. Health, Part A: Toxic/Hazard. Subst. Environ. Eng. 40 (2), 265–287.

Stapleton, H.M., Sharma, S., Getzinger, G., Ferguson, P.L., Gabriel, M., Webster, T.F., Blum, A., 2012. Novel and high volume use flame retardants in US couches reflective of the 2005 pentaBDE phase out. Environ. Sci. Technol. 46 (24), 13432–13439.

Statista Research Department, 2023. June 12. https://www.statista.com/statistics/282732/global-production-of-plastics-since-1950/.

Sutton, R., Chen, D., Sun, J., Greig, D.J., Wu, Y., 2019. Characterization of brominated, chlorinated, and phosphate flame retardants in San Francisco Bay, an urban estuary. Sci. Total Environ. 652, 212–223. https://doi.org/10.1016/j.scitotenv.2018.10.096.

Tena, A., Piégay, H., Seignemartin, G., Barra, A., Berger, J.F., Mourier, B., Winiarski, T., 2020. Cumulative effects of channel correction and regulation on floodplain terrestrialisation patterns and connectivity. Geomorphology 354, 107034. https://doi.org/10.1016/j.geomorph.2020.107034.

USEPA, 1986. EPA Regulation 40 CFR Part 136 (Appendix B) Appendix B to Part 136 D Definition and Procedure for the Determination of the Method Detection Limited Revision 1.11. US Environmental Protection Agency (EPA). Available at: http://www.ecfr.gov/. (Accessed 5 March 2013).

van der Veen, I., de Boer, J., 2012. Phosphorus flame retardants: properties, production environmental occurrence, toxicity and analysis. Chemosphere 88, 1119–1153. https://doi.org/10.1016/j.chemosphere.2012.03.067.

Wang, X., Zhu, Q.Q., Yan, X.T., Wang, Y.W., Liao, C.Y., Jiang, G.B., 2020. A review of organophosphate flame retardants and plasticizers in the environment: analysis, occurrence and risk assessment. Sci. Total Environ. 731, 139071. https://www.10.1016/j.scitotenv.2020.139071.

Wei, G.L., Li, D.Q., Zhuo, M.N., Liao, Y.S., Xie, Z.Y., Guo, T.L., Li, J.J., Zhang, S.Y., Liang, Z.Q., 2015. Organophosphorus flame retardants and plasticizers: sources, occurrence, toxicity and human exposure. Environ. Pollut. 196, 29–46. https://doi.org/10.1016/j.envpol.2014.09.012.

Xiang, L., Wang, X.D., Chen, X.H., Mo, C.H., Li, Y.W., Li, H., Cai, Q.Y., Zhou, D.M., Wong, M.H., Li, Q.X., 2019. Sorption mechanism, kinetics, and isotherms of di-n-butyl phthalate to different soil particle-size fractions. J. Agric. Food Chem. 67, 4734–4745. https://www.10.1021/acs.jafc.8b0635.

Xu, X.R., Li, X.Y., 2008. Adsorption behaviour of dibutyl phthalate on marine sediments. Mar. Pollut. Bull. 57, 403–408. https://doi.org/10.1016/j.marpolbul.2008.01.023.

Yang, J., Zhao, Y., Li, M., Du, M., Li, X., Li, Y., 2019. A review of a class of emerging contaminants: the classification, distribution, intensity of consumption, synthesis routes, environmental effects and expectation of pollution abatement to organophosphate flame retardants (OPFRs). Int. J. Mol. Sci. 20, 1–38. https://doi.org/10.3390/ijms20122874.

Zhang, H., Zhou, Q., Xie, Z., Zhou, Y., Tu, C., Fu, C., Mi, W., Ebinghaus, R., Christie, P., Luo, Y., 2018. Occurrences of organophosphorus esters and phthalates in the microplastics from the coastal beaches in north China. Sci. Total Environ. 616–617, 1505–1512. https://doi.org/10.1016/j.scitotenv.2017.10.163.

Eyrolle, F., Boyer, P., Chaboche, P.A., De Vismes, A., Lepage, H., Seignemartin, G., Mourier, B., et al. Temporal Trajectories of Artificial Radiocaesium 137Cs in French Rivers over the Nuclear Era Reconstructed from Sediment Cores. Scientific reports. submitted for publication. Submitted.